Published in final edited form as:
Toxicol Appl Pharmacol. 2014 September 15; 279(3): 266–274. doi:10.1016/j.taap.2014.05.010.

Mechanisms of Acetaminophen-induced Cell Death in Primary Human Hepatocytes

Yuchao Xie[1], **Mitchell R. McGill**[1], **Kenneth Dorko**[1], **Sean C. Kumer**[2], **Timothy M. Schmitt**[2], **Jameson Forster**[2], and **Hartmut Jaeschke**[1,*]

[1]Department of Pharmacology, Toxicology and Therapeutics, University of Kansas Medical Center, Kansas City, KS 66160

[2]Department of Surgery, University of Kansas Medical Center, Kansas City, KS 66160

Abstract

Acetaminophen (APAP) overdose is the most prevalent cause of drug-induced liver injury in western countries. Numerous studies have been conducted to investigate the mechanisms of injury after APAP overdose in various animal models; however, the importance of these mechanisms for humans remains unclear. Here we investigated APAP hepatotoxicity using freshly isolated primary human hepatocytes (PHH) from either donor livers or liver resections. PHH were exposed to 5mM, 10mM or 20mM APAP over a period of 48 hours and multiple parameters were assessed. APAP dose-dependently induced significant hepatocyte necrosis starting from 24h, which correlated with the clinical onset of human liver injury after APAP overdose. Interestingly, cellular glutathione was depleted rapidly during the first 3h. APAP also resulted in early formation of APAP-protein adducts (measured in whole cell lysate and in mitochondria) and mitochondrial dysfunction, indicated by the loss of mitochondrial membrane potential after 12h. Furthermore, APAP time-dependently triggered c-Jun N-terminal kinase (JNK) activation in the cytosol and translocation of phospho-JNK to the mitochondria. Both co-treatment and post-treatment (3h) with the JNK inhibitor SP600125 reduced JNK activation and significantly attenuated cell death at 24h and 48h after APAP. The clinical antidote N-acetylcysteine offered almost complete protection even if administered 6 hours after APAP and a partial protection when given at 15h. Conclusion: These data highlight important mechanistic events in APAP toxicity in PHH and indicate a critical role of JNK in the progression of injury after APAP in humans. The JNK pathway may represent a therapeutic target in the clinic.

[*]**For Correspondence:** Dr. Hartmut Jaeschke, Department of Pharmacology, Toxicology & Therapeutics, University of Kansas Medical Center, 3901 Rainbow Blvd, MS 1018, Kansas City, KS 66160, Tel +1 913 588 7969, Fax +1 913 588 7501, hjaeschke@kumc.edu.

CONFLICT OF INTEREST DISCLOSURE
The authors declare no competing financial interest.

Keywords

Drug-induced liver injury; acetaminophen protein adducts; oncotic necrosis; c-Jun-N-terminal kinase; mitochondrial dysfunction

Introduction

Acetaminophen (APAP; paracetamol) is widely used as an analgesic and antipyretic drug. At therapeutic doses, it is considered effective and safe but an overdose can cause severe liver injury, liver failure and even death (Larson, 2007). Currently, APAP is the leading cause of drug-induced liver failure in the US and UK (Lee, 2012). Considerable progress has been made in the understanding of the mechanisms of injury after APAP overdose in animal models (McGill and Jaeschke, 2013; Jaeschke et al., 2012). Although most of the drug is conjugated with glucuronic acid or sulfate and excreted, a small fraction is metabolized by cytochrome P450 enzymes to a reactive metabolite, presumably *N*-acetyl-*p*-benzoquinone imine (NAPQI). NAPQI can be scavenged through conjugation with glutathione (GSH) and can react with protein sulfhydryl groups to form adducts (Mitchell et al., 1973) It is thought that protein adducts, especially in mitochondria, cause mitochondrial dysfunction and an early oxidant stress, which initiates the activation of various MAP kinases (Jaeschke et al., 2012). Ultimately, the activities of different kinases converge to phosphorylate c-jun-N-terminal kinase (P-JNK), which then translocates to the mitochondria and amplifies the oxidant stress and peroxynitrite formation (Hanawa et al., 2008; Saito et al., 2010a). This mitochondrial oxidant stress leads to the opening of the membrane permeability transition (MPT) pore with collapse of the membrane potential and cessation of ATP synthesis. In addition, the MPT causes mitochondrial matrix swelling, with rupture of the outer membrane and the release of intermembrane proteins, such as endonuclease G and apoptosis-inducing factor, which translocate to the nucleus and induce DNA fragmentation (Jaeschke et al., 2012). Together, these events result in cell necrosis (Gujral et al., 2002).

After the early mechanistic insight into APAP hepatotoxicity in mice leading to the development of the first clinical antidote N-acetylcysteine (NAC) (Prescott et al., 1977), no further therapeutic intervention has been developed during the last 35 years. One of the main reasons is limited understanding of the human pathophysiology, which makes it difficult to directly extrapolate potential therapeutic targets in mice to humans. However, some progress has been made recently. In the metabolically competent human hepatoma cell line HepaRG, APAP-induced protein adduct formation, mitochondrial dysfunction and oxidant stress preceded cell necrosis at 24–48h (McGill et al., 2011). In patients with APAP overdose, high levels of protein adducts have been detected in serum (Muldrew et al., 2002; Davern et al., 2006). Furthermore, evidence for mitochondrial damage, i.e. the leakage into serum of the mitochondrial matrix enzyme glutamate dehydrogenase (GDH) and mitochondrial DNA, were measured in patients with liver injury (McGill et al., 2012a). The rise of serum acylcarnitines reflected mitochondrial dysfunction in mice; however, this effect was not observed in humans because of the suppression by the standard of care NAC treatment (McGill et al., 2014b). In addition, cell death markers and damage associated molecular patterns found in mice, such as high mobility group box 1 protein, microRNA-122,

cytokeratin-18, nuclear DNA fragments, and argininosuccinate synthetase, were also observed in serum of patients (McGill et al., 2012a, 2014a; Antoine et al., 2012, Starkey-Lewis et al., 2011). Despite these similarities in cellular responses to APAP overdose in mice and in humans, detailed signaling mechanisms of APAP-induced cell death in human hepatocytes remain unclear. A better understanding of these events is critical for development of any additional therapeutic interventions. Therefore, the aim of the present study was to investigate the mechanisms of hepatotoxicity of APAP in freshly isolated primary human hepatocytes (PHH). Specifically, we wanted to determine critical but as yet unexplored events in PHH such as mitochondrial protein binding, mitochondrial dysfunction and mitochondrial translocation of P-JNK. Our data show similarities but also essential differences to mouse hepatocytes, some of which may explain the delayed toxicity in humans and PHH.

Materials and Methods

Isolation of primary human hepatocytes

All human tissues were obtained with informed consent from each patient, according to ethical and institutional guidelines. The study was approved by the University of Kansas Medical Center Institutional Review Board. A summary of medical information of donors is provided in Table 1. No donor tissue was obtained from executed prisoners or other institutionalized persons. All liver specimens were obtained in accordance with a Human Subject Committee approved protocol from patients undergoing a hepatic resection procedure or from donor organs. Liver specimens were obtained from the hospital operating room and placed in a sterile container that contains either cold sterile saline or cold University of Wisconsin's (UW) solution. The liver specimens were then placed in a secondary container with ice and transported back to the cell isolation lab. Once in the lab, all procedures were then performed in a biological safety cabinet using aseptic technique. A pan of ice was placed in the biological safety cabinet and covered by a plastic bag and then a sterile field was placed over the bag. The liver specimen was then placed on top of the sterile field. Catheters were inserted into the major portal and/or hepatic vessels and the tissue was perfused with cold EMEM (Mediatech cat # 15-010-CM) containing 25 mM HEPES buffer (Mediatech cat # 25–060-CI) to determine which vessels provide the most uniform perfusion of the tissue. The catheters were then secured into the vessels either by sutures or surgical grade glue. All remaining major vessels on the cut surfaces were closed with sutures and/or surgical grade glue. The liver tissue was then placed in a sterile plastic bag and connected to a peristaltic pump with the flow rate dependent on the number of catheters and size of tissue. The bag containing the tissue was placed in a water bath at 37°C and the tissue was perfused with calcium, magnesium and phenol red free HBSS (Hyclone cat # SH30588.02) containing EGTA (1.0 mM) without recirculation for 10–15 minutes. The EGTA chelates calcium which leads to the separation of cell junctions and helps to remove any residual blood. The liver specimen was then perfused for 8–10 minutes using HBSS without EGTA to flush residual EGTA from the tissue. Finally, the liver specimen was perfused with EMEM containing 0.1 mg/ml of collagenase (VitaCyte cat# 001–2030) and 0.02 mg/ml of protease (VitaCyte cat# 003–1000) which was recirculated as long as needed (18–30 min.) to complete the digestion. All perfusion solutions were maintained at

37°C via a water bath. Perfusion of the specimen was stopped when the liver tissue began to show fissures and separation from the liver capsule. The liver tissue was then removed from the plastic bag and placed in a sterile plastic beaker that contains ice-cold EMEM + 25 mM HEPES. The specimen was then gently chopped with sterile scissors to release hepatocytes. The cell suspension was filtered through sterile gauze-covered funnels to remove cellular debris and clumps of undigested tissue. Hepatocytes were isolated from the other cell types in the suspension by low speed centrifugation at 80g for 5 min at 40°C. The supernatant was decanted and the centrifugation steps were repeated 2 more times using cold EMEM + 25 mM HEPES to re-suspend the hepatocytes after each spin. After three washes in EMEM + 25 mM HEPES, the hepatocytes were re-suspended in cold Williams' Medium E (Life Technologies cat # A12176-01 supplemented with L-Glutamine (2 mM) (Life Technologies cat # 35050-061), HEPES (10 mM), insulin (10-7M) dexamethasone (10-7M), penicillin (100 U/ml), streptomycin (100μg/ml) and amphotericin B (0.25μg/ml). Cell viability was assessed by trypan blue exclusion and cell number was determined by using a hemocytometer viewed through an inverted microscope. Viabilities were expressed as a percentage of the total cell number. The hepatocytes were brought to a concentration of 0.5×10^6 cells/ml in Williams' Medium E, as described above, plus 5% bovine calf serum. The hepatocytes were then seeded on collagen coated plates and allowed to attach in a humidified 37°C, 5% CO_2 incubator for 2–12 hours and then the medium was changed to serum free Williams' Medium E supplemented as described.

Primary human hepatocytes experiments

Approximately 3 h after being seeded on collagen-coated dishes, cells were washed with sterile phosphate-buffered saline (PBS) and treated with APAP dissolved in Hepatocyte Maintenance Medium (Lonza, Walkersvill, MD) supplemented with insulin, dexamethasone, and gentamicin/amphotericin-B. Due to the limited number of hepatocytes obtained from each isolation procedure it is not possible to perform a complete set of assays on each batch of hepatocytes. We did not specifically assign patients to certain experiments. However, for every batch of cells, we measured ALT release of hepatocytes 24 and 48h after 10 mM APAP to make sure the cells are responding properly. For JNK inhibitor treatment, SP600125 (Calbiochem, Darmstadt, Germany) dissolved in dimethyl sulfoxide (DMSO) was added to the cell culture medium to achieve a final concentration of 10μM, either at the same time as APAP treatment, or 3h afterwards . For caspase inhibition experiments, cells were co-treated with 20μM of Z-VD-fmk (generous gift from Dr. S.X.Cai, Epicept, San Diego, CA) and APAP. For N-acetylcysteine (NAC) treatment, NAC was dissolved in H_2O and then added to the culture medium at a series of time points after APAP to achieve the final concentration of 20mM.

APAP-protein adducts measurement

APAP-protein adducts were measured in total cell homogenate and in mitochondria. Briefly, hepatocytes or isolated mitochondria were lysed in 10mM sodium acetate buffer, pH 6.5, by brief sonication or several cycles of freeze-thaw, respectively, and the lysates were filtered through a size exclusion column (Biospin-6 columns, Bio-Rad Laboratories, Hercules, CA) to remove low molecular weight compounds. The purified proteins were then digested overnight with proteases. Proteases were precipitated with an acetone/methanol mixture and

pelleted, and the supernatants evaporated to a residue. The residue was then dissolved in 50μL sodium acetate buffer and subjected to high pressure liquid chromatography with electrochemical detection (HPLC-ECD) of protein-derived APAP-cysteine (Muldrew et al., 2002; McGill et al., 2013). Protein in the lysates was measured using the bicinchoninic acid assay (BCA).

Biochemical assays

ALT levels were determined using an ALT reagent kit (Pointe Scientific, MI). GDH activity was evaluated as described (McGill et al., 2012a). Using Ac-DEVD-AMC as the substrate, caspase-3 activity was measured as previously described in detail (Jaeschke et al., 1998). A modified method of the Tietze assay was carried out to measure cellular glutathione levels as described (Jaeschke and Mitchell, 1990). To detect the mitochondrial membrane potential, JC-1 Mitochondrial Membrane Potential Kit (Cell Technology, Mountain View, CA) was used as described in detail (Bajt et al., 2004).

PI staining

PHH were allowed to adhere on glass bottom dishes for 3 hours, followed by 10mM APAP. The medium was removed after 24h and cells were stained with 500nM of propidium iodide (Invitrogen) for 5 min. Nuclei were stained with 4',6-diamidino-2-phenylindole (DAPI) and images were recorded with a fluorescence microscope.

Isolation of subcellular fractions and western blotting

Mitochondria and cytosolic fractions were isolated from cell lysates using differential centrifugation as described (Cover et al., 2005). Standard western blotting was performed using a rabbit anti-JNK antibody and a rabbit anti-phospho-JNK antibody (Cell Signaling Technology, Danvers, MA).

HepaRG cells

HepaRG cells were differentiated and treated as described (McGill et al., 2011).

Statistics

All results were expressed as mean ± standard error (SE). Comparisons between multiple groups were performed with one-way ANOVA followed by post hoc Student-Newman-Keuls test. If the data were not normally distributed, the Kruskal-Wallis Test was used (nonparametric ANOVA) followed by Dunn's Multiple Comparisons Test. $P < 0.05$ was considered significant.

Results

APAP induces necrotic cell death in PHH

We evaluated the toxicity of APAP in freshly isolated PHH by performing a time course study with 5mM and 10mM APAP. APAP resulted in significant cellular ALT release into the culture medium starting from 24h with a progressive further increase up to 48h (Fig. 1A). The injury was dose-dependent (Fig. 1B). PI staining of the nuclei confirmed the

necrotic cell death (Fig 1C). Furthermore, no increase in caspase-3 activity was detectable in APAP-treated PHH cells at 24h (data not shown).

The total number of cell isolations for this manuscript was 44 with the donor patient information listed in Table 1. For each batch, cell injury was determined at 24 and 48h after APAP exposure and compared to cell death in controls. Figure 2A demonstrates the variability in the cell death response between different batches of cells. In addition, the groups were separated into cells from male and female donors (Figure 2B). Our results do not indicate a statistically significant gender difference in toxicity in response to APAP exposure. Furthermore, GSH depletion of cells from 7 individual donors is shown in Figure 2C. Together, these data demonstrate a limited inter-individual variability in APAP-induced toxicity between cells from different donors.

APAP triggers GSH depletion, mitochondria dysfunction and protein adducts formation in PHH

APAP is metabolized to the electrophile NAPQI, which can react with the sulfhydryl groups of cysteine in GSH or cellular proteins. Exposure to 10mM APAP reduced cellular GSH levels by >70% within 3h, followed by further depletion over the next 20h (Fig. 3A). Measurement of the mitochondrial membrane potential with the JC-1 assay revealed significant mitochondrial dysfunction and loss of mitochondrial membrane potential between 6 and 15h after APAP (Fig. 3B). Protein adducts in the cells were formed mainly during the first 6h, with no further increase up to 15h (Fig. 3C). Interestingly, protein adducts in mitochondria did not increase during the first 3h, i.e. before GSH was depleted by 70%. However, mitochondrial adduct levels dramatically increased between 3 and 6h (Fig. 3D). These time course experiments revealed a sequence of events in PHH after APAP exposure that includes rapid GSH depletion and protein adduct formation, with mitochondrial protein adduct formation and mitochondrial dysfunction occurring later, only after extensive GSH depletion.

APAP causes JNK activation and mitochondrial translocation in PHH

JNK activation and the mitochondrial translocation of phospho-JNK (P-JNK) have been well established as a second hit in mouse hepatocytes to amplify the initial oxidative stress (Hanawa et al., 2008; Saito et al., 2010a). To explore the role of JNK in PHH, APAP-treated cells were harvested at several time points and the lysates were probed for JNK and P-JNK by western blotting. APAP resulted in time-dependent JNK activation which was first detectable at 6h, with progressive decrease subsequently (Fig. 4A). This result was confirmed by densitometry and the calculation of the P-JNK-to-JNK ratio (Fig. 4B). To determine whether activated JNK translocated into mitochondria as it does in mouse hepatocytes, cytosolic and mitochondrial fractions were isolated from PHH and JNK activation was evaluated at 6 and 15h after APAP treatment. Similar to what was observed in total cell lysate, APAP exposure caused JNK activation in the cytosol at 6 and 15h (Fig. 4C). Some JNK (mainly 54kDa) was observed in mitochondria from controls, with a modest but significant increase in P-JNK 6h after APAP exposure and massive P-JNK at 15h (Fig. 4C). These results were confirmed by densitometry and the calculation of the P-JNK-to-JNK ratio (Fig. 4D).

JNK inhibitor SP600125 partially protects against APAP-induced cell death in PHH

Given the beneficial effect of the JNK inhibitor SP600125 in animals, we sought to determine whether it protects against APAP in PHH. Cells were treated with SP600125 either simultaneously with APAP or 3h after APAP, and cell death was evaluated at 24 and 48h. As SP600125 was dissolved in DMSO, a well-known inhibitor of cytochrome P450 enzymes, the concentration of SP600125 was limited to 10μM to reduce interference with APAP metabolism. Despite this low concentration, SP600125 consistently reduced cell death at both time points and with both treatment paradigms (Fig. 5A, B). To verify the ability of SP600125 to inhibit JNK activation in human hepatocytes, western blotting was conducted. Treatment with this low concentration of SP600125 moderately lowered the activation of JNK in both co-treated and post-treated cells without altering total JNK levels (Fig. 5C). Thus, JNK is involved in the progression of cell death after APAP in PHH.

JNK is not relevant for APAP-induced cell death in HepaRG cells

Previous data have demonstrated that HepaRG cells, a bipotent human hepatoma cell line, are a useful model to study APAP hepatotoxicity (McGill et al., 2011). For comparison, JNK activation in HepaRG cells was evaluated. Over a period of 24h, JNK activation was barely detectable after APAP treatment, and total JNK levels remained almost constant (Fig. 6A). Surprisingly, co-treatment of SP600125 with APAP aggravated the injury rather than preventing it (Fig. 6B). Based on these data, JNK activation does not appear to be relevant for cell death after APAP in HepaRG cells.

Protection against APAP-induced cell death in PHH by the clinical antidote N-acetylcysteine

To test if NAC is able to reduce APAP toxicity in PHH, cells were treated with 10mM APAP and 20mM NAC at the same time or 3–24h after APAP. APAP alone caused 29% and 68% cell death at 24 and 48h, respectively (Fig. 7A). NAC treatment completely prevented cell death at 24h when given up to 6h after APAP and significantly attenuated ALT release by 77% at 48h (Fig. 7A). There was still a trend of reduced ALT release at 48h when the cells were treated with NAC at 15h. However, the protection by NAC was completely lost in the 24h post-treatment group (Fig. 7A). When GDH as indicator for mitochondrial dysfunction was measured, NAC given either at the same time or 6h after APAP totally eliminated the release of GDH at 24 or 48h after APAP exposure (Fig. 7B). Furthermore, NAC treatment eliminated JNK activation at 24h (Fig. 7C,D).

Discussion

The aim of this investigation was to elucidate intracellular mechanisms of cell death after APAP in primary human hepatocytes. Importantly, we used freshly isolated cells. The hepatocytes were exposed to APAP immediately after isolation from fresh tissue and adherence to the tissue culture plates. Focusing on known events in murine hepatocytes, we observed similarities but also relevant differences between human and mouse cells which need to be considered when new therapeutic strategies are discussed.

GSH depletion and protein adducts

The electrophilic metabolite NAPQI reacts rapidly with GSH, causing extensive GSH depletion in mouse livers *in vivo* (>80% within 30 min) (McGill et al., 2013) and in cultured mouse hepatocytes (>80% within 3h) (Bajt et al., 2004). Compared to the much more delayed GSH depletion in the metabolically competent human hepatoma cell line HepaRG (McGill et al., 2011), PHH responded very similar to mouse hepatocytes with a rapid GSH depletion of >70% within 3h. In addition, extensive protein adduct formation was observed in PHH with peak levels at 6h. APAP protein adducts in mice and mouse hepatocytes peak around 2h and 3h, respectively (McGill et al., 2012b, 2013). More importantly, protein adducts in mitochondria, which are thought to initiate mitochondrial dysfunction, also peak at the same time in mouse cells (McGill et al., 2013; Xie et al., 2013). However, mitochondrial protein formation was delayed in PHH compared to mouse hepatocytes and dramatically increased mainly after GSH depletion. Interestingly, on the basis of mg protein, APAP-Cys adducts levels were 1.5-to-3-times higher in PHH than in mouse hepatocytes or livers *in vivo*. Thus, while GSH depletion and total protein binding in response to APAP is only minimally delayed compared to mouse hepatocytes, two fundamental differences between PHH and mice are the delayed mitochondrial protein adduct formation and the overall higher protein binding in human cells. A potential reason for the different time line in mitochondrial adduct formation could be an involvement of mitochondrial cyp2e1 in the process (Knockaert et al., 2011). However, further studies are required to investigate this hypothesis in detail.

Mitochondrial dysfunction and JNK activation

It is generally accepted that the early protein adduct formation in mouse hepatocytes leads to mitochondrial oxidant stress, which triggers the activation of several MAP kinases, including apoptosis signal-regulating kinase 1 (Nakagawa et al., 2008), mixed lineage kinase 3 (Sharma et al., 2012), receptor interacting protein kinases 1and 3 (Ramachandran et al., 2013; Zhang et al., 2014), and glycogen synthase kinase-3 beta (Shinohara et al., 2010), all of which are thought to eventually trigger the downstream phosphorylation of JNK. P-JNK then translocates into mitochondria (Hanawa et al., 2008) and amplifies the mitochondrial oxidant stress (Saito et al., 2010a) to a level that can trigger MPT pore opening and cell necrosis (Kon et al., 2004). In PHH, JNK activation in the cytosol was delayed for several hours compared to mice, consistent with the delayed mitochondrial protein adduct formation. In addition, the mitochondrial translocation of P-JNK, which can be observed within 2–3h after APAP exposure in mice (Hanawa et al., 2008; McGill et al., 2012b), was even more delayed in PHH. P-JNK translocation to mitochondria correlated with the collapse of the mitochondrial membrane potential followed by the onset of cell necrosis. Thus, many events observed in mouse hepatocytes in response to APAP also occur in PHH, but most of these events are substantially delayed and this may explain the delayed onset of necrosis in humans.

The critical role of JNK activation as an amplification system in the pathophysiology of APAP hepatotoxicity has been demonstrated by the protection provided by the JNK inhibitor SP600125 or knock-down of JNK genes *in vivo* (Gunawan et al., 2006; Henderson et al., 2007). In contrast, the JNK inhibitor was only partially effective in cultured mouse

hepatocytes, and only in the presence of the GSH synthesis inhibitor BSO (Gunawan et al., 2006). We have confirmed that the inhibitor was ineffective in protecting against APAP-induced cell death in cultured mouse hepatocytes (Y Xie and H Jaeschke, unpublished). Thus, the partial protection in PHH by SP600125 suggests that JNK activation is an important step in the pathophysiology in humans. However, the concentration of the inhibitor used in our experiments was sub-optimal. A limitation of SP600125 is the need to use DMSO as solvent, which can prevent APAP-induced hepatotoxicity due to inhibition of P450 enzymes even at very low concentrations and thus protect through off-target effects (Jaeschke et al., 2006). Interestingly, APAP did not cause JNK activation and SP600125 did not protect against APAP toxicity in HepaRG cells. Although we cannot rule out the possibility that hepatoma cells have altered signaling mechanisms, another explanation could be that other signaling pathways besides JNK are involved in the progression of injury. Recent data suggest that protein kinase C (PKC) inhibitors alleviated APAP-induced liver injury both *in vivo* and *in vitro* (Saberi et al., 2014). However, a classical PKC inhibitor and knocking down of PKC-α protected through inhibition of JNK while broad-spectrum PKC inhibitors protected through a JNK-independent but AMPK-dependent pathway (Saberi et al., 2014). Preventing phosphorylation of AMPK by these PKC inhibitors led to activation of survival pathways such as autophagy (Saberi et al., 2014), which removes damaged mitochondria and protects against APAP-induced hepatotoxicity (Ni et al., 2012). Thus, the JNK pathway is an important amplification mechanism that aggravates the oxidant stress and promotes APAP-induced cell death in murine and human hepatocytes but PKC-mediated signaling independent of JNK may also contribute to the pathophysiology.

Protection by the clinical antidote N-acetylcysteine in PHH

For more than 35 years, NAC has been the only clinically approved antidote against APAP poisoning (Polson and Lee, 2005). NAC is most effective when given within 8h of APAP overdose, but has been shown to be partially beneficial even when administered up to 24h after APAP exposure (Smilkstein et al., 1988). The mechanism of protection during the early, metabolism phase primarily involves improved scavenging of the reactive metabolite NAPQI due to accelerated GSH synthesis (Corcoran et al., 1985), while the later effects include scavenging of mitochondrial oxidant stress and support of mitochondrial energy metabolism (Saito et al., 2010b). The experiments with delayed NAC treatment of PHH demonstrated complete protection up to 6h after APAP, and partial protection when the cells were treated at 15h. These results closely resemble the clinical effectiveness of NAC. In contrast, delayed NAC treatment in mice or mouse hepatocytes is not effective beyond 2h after APAP exposure, underscoring the much more accelerated pathophysiology in the murine systems. Thus, despite the usefulness of mice and mouse hepatocytes to study APAP-induced cell death, our results demonstrate that freshly isolated PHH are clearly superior to animal models and human cell lines.

In summary, our results demonstrated rapid GSH depletion, formation of cellular and mitochondrial protein adducts, JNK activation and P-JNK translocation to mitochondria, loss of the mitochondrial membrane potential and cell necrosis in PHH after APAP exposure. Although the overall sequence of events was similar to mouse hepatocytes, there was clearly a substantial delay in formation of mitochondrial protein adducts, which

occurred mainly after extensive GSH depletion. Similarly, JNK activation and translocation to the mitochondria were delayed. These events triggered the later loss of the mitochondrial membrane potential and cell necrosis. In addition, JNK inhibition was partially effective in PHH. Furthermore, NAC post-treatment was completely protective in PHH when administered as late as 6h, and partially effective up to 15h, after APAP. Overall, this timeline of APAP-induced cell death in PHH is very close to events observed in APAP overdose patients. Therefore, we can conclude that freshly isolated PHH are the best available model to study mechanisms of APAP-induced cell death and are the most relevant model for the human pathophysiology. Mouse hepatocytes or mice *in vivo* share many similarities with PHH, but differences in the time line of cell death and potentially in the details of signaling events are emerging. This means that it will be important to use PHH to test new therapeutic targets discovered in murine models before contemplating translating these findings into the clinic.

Acknowledgments

This work was supported in part by grants from the University of Kansas Medical Center Liver Center (to H.J.), from the National Institutes of Health (R01 DK070195 and R01 AA12916) (to H.J.), and from the National Center for Research Resources (5P20RR021940-07) and the National Institute of General Medical Sciences (8 P20 GM103549-07) of the National Institutes of Health. Additional support came from the “Training Program in Environmental Toxicology” T32 ES007079-26A2 (to M.R.M.) from the National Institute of Environmental Health Sciences.

REFERENCES

Antoine DJ, Jenkins RE, Dear JW, Williams DP, McGill MR, Sharpe MR, Craig DG, Simpson KJ, Jaeschke H, Park BK. Molecular forms of HMGB1 and keratin-18 as mechanistic biomarkers for mode of cell death and prognosis during clinical acetaminophen hepatotoxicity. J Hepatol. 2012; 56:1070–1079. [PubMed: 22266604]

Bajt ML, Knight TR, Lemasters JJ, Jaeschke H. Acetaminophen-induced oxidant stress and cell injury in cultured mouse hepatocytes: protection by N-acetyl cysteine. Toxicol Sci. 2004; 80:343–349. [PubMed: 15115886]

Corcoran GB, Racz WJ, Smith CV, Mitchell JR. Effects of N-acetylcysteine on acetaminophen covalent binding and hepatic necrosis in mice. J Pharmacol Exp Ther. 1985; 232:864–872. [PubMed: 3973835]

Cover C, Mansouri A, Knight TR, Bajt ML, Lemasters JJ, Pessayre D, Jaeschke H. Peroxynitrite-induced mitochondrial and endonuclease-mediated nuclear DNA damage in acetaminophen hepatotoxicity. J Pharmacol Exp Ther. 2005; 315:879–887. [PubMed: 16081675]

Davern, TJ2nd; James, LP.; Hinson, JA.; Polson, J.; Larson, AM.; Fontana, RJ.; Lalani, E.; Munoz, S.; Shakil, AO.; Lee, WM. Acute Liver Failure Study Group. Measurement of serum acetaminophen-protein adducts in patients with acute liver failure. Gastroenterology. 2006; 130:687–694. [PubMed: 16530510]

Gujral JS, Knight TR, Farhood A, Bajt ML, Jaeschke H. Mode of cell death after acetaminophen overdose in mice: apoptosis or oncotic necrosis? Toxicol Sci. 2002; 67:322–328. [PubMed: 12011492]

Gunawan BK, Liu ZX, Han D, Hanawa N, Gaarde WA, Kaplowitz N. c-Jun N-terminal kinase plays a major role in murine acetaminophen hepatotoxicity. Gastroenterology. 2006; 131:165–178. [PubMed: 16831600]

Hanawa N, Shinohara M, Saberi B, Gaarde WA, Han D, Kaplowitz N. Role of JNK translocation to mitochondria leading to inhibition of mitochondria bioenergetics in acetaminophen-induced liver injury. J Biol Chem. 2008; 283:13565–13577. [PubMed: 18337250]

Henderson NC, Pollock KJ, Frew J, Mackinnon AC, Flavell RA, Davis RJ, Sethi T, Simpson KJ. Critical role of c-jun (NH2) terminal kinase in paracetamol- induced acute liver failure. Gut. 2007; 56:982–990. [PubMed: 17185352]

Jaeschke H, Cover C, Bajt ML. Role of caspases in acetaminophen-induced liver injury. Life Sci. 2006; 78:1670–1676. [PubMed: 16226279]

Jaeschke H, Fisher MA, Lawson JA, Simmons CA, Farhood A, Jones DA. Activation of caspase 3 (CPP32)-like proteases is essential for TNF-alpha-induced hepatic parenchymal cell apoptosis and neutrophil-mediated necrosis in a murine endotoxin shock model. J Immunol. 1998; 160:3480–3486. [PubMed: 9531309]

Jaeschke H, McGill MR, Ramachandran A. Oxidant stress, mitochondria, and cell death mechanisms in drug-induced liver injury: lessons learned from acetaminophen hepatotoxicity. Drug Metab Rev. 2012; 44:88–106. [PubMed: 22229890]

Jaeschke H, Mitchell JR. Use of isolated perfused organs in hypoxia and ischemia/reperfusion oxidant stress. Methods Enzymol. 1990; 186:752–759. [PubMed: 2233332]

Knockaert L, Descatoire V, Vadrot N, Fromenty B, Robin MA. Mitochondrial CYP2E1 is sufficient to mediate oxidative stress and cytotoxicity induced by ethanol and acetaminophen. Toxicol In Vitro. 2011; 25:475–484. [PubMed: 21130154]

Kon K, Kim JS, Jaeschke H, Lemasters JJ. Mitochondrial permeability transition in acetaminophen-induced necrosis and apoptosis of cultured mouse hepatocytes. Hepatology. 2004; 40:1170–1179. [PubMed: 15486922]

Larson AM. Acetaminophen hepatotoxicity. Clin Liver Dis. 2007; 11:525–548. [PubMed: 17723918]

Lee WM. Acute liver failure. Semin Respir Crit Care Med. 2012; 33:36–45. [PubMed: 22447259]

McGill MR, Cao M, Svetlov A, Sharpe MR, Williams CD, Curry SC, Farhood A, Jaeschke H, Svetlov SI. Argininosuccinate synthetase is an early plasma biomarker of liver injury and active cell death during acetaminophen hepatotoxicity in mice and humans. Biomarkers. 2014a; 19:222–230. [PubMed: 24597531]

McGill MR, Jaeschke H. Metabolism and disposition of acetaminophen: recent advances in relation to hepatotoxicity and diagnosis. Pharm Res. 2013; 30:2174–2187. [PubMed: 23462933]

McGill MR, Lebofsky M, Norris HR, Slawson MH, Bajt ML, Xie Y, Williams CD, Wilkins DG, Rollins DE, Jaeschke H. Plasma and liver acetaminophen-protein adduct levels in mice after acetaminophen treatment: dose-response, mechanisms, and clinical implications. Toxicol Appl Pharmacol. 2013; 269:240–249. [PubMed: 23571099]

McGill MR, Li F, Sharpe MR, Williams CD, Curry SC, Ma X, Jaeschke H. Circulating acylcarnitines as biomarkers of mitochondrial dysfunction after acetaminophen overdose in mice and humans. Arch Toxicol. 2014b; 88:391–401. [PubMed: 23979652]

McGill MR, Sharpe MR, Williams CD, Taha M, Curry SC, Jaeschke H. The mechanism underlying acetaminophen-induced hepatotoxicity in humans and mice involves mitochondrial damage and nuclear DNA fragmentation. J Clin Invest. 2012a; 122:1574–1583. [PubMed: 22378043]

McGill MR, Williams CD, Xie YC, Ramachandran A, Jaeschke H. Acetaminophen-induced liver injury in rats and mice: Comparison of protein adducts, mitochondrial dysfunction, and oxidative stress in the mechanism of toxicity. Toxicol Appl Pharmacol. 2012b; 264:387–394. [PubMed: 22980195]

McGill MR, Yan HM, Ramachandran A, Murray GJ, Rollins DE, Jaeschke H. HepaRG cells: a human model to study mechanisms of acetaminophen hepatotoxicity. Hepatology. 2011; 53:974–982. [PubMed: 21319200]

Mitchell JR, Jollow DJ, Potter WZ, Gillette JR, Brodie BB. Acetaminophen-induced hepatic necrosis. IV. Protective role of glutathione. J Pharmacol Exp Ther. 1973; 187:211–217. [PubMed: 4746329]

Muldrew KL, James LP, Coop L, McCullough SS, Hendrickson HP, Hinson JA, Mayeux PR. Determination of acetaminophen-protein adducts in mouse liver and serum and human serum after hepatotoxic doses of acetaminophen using high-performance liquid chromatography with electrochemical detection. Drug Metab Dispos. 2002; 30:446–451. [PubMed: 11901099]

Nakagawa H, Maeda S, Hikiba Y, Ohmae T, Shibata W, Yanai A, Sakamoto K, Ogura K, Noguchi T, Karin M, Ichijo H, Omata M. Deletion of apoptosis signal-regulating kinase 1 attenuates

acetaminophen-induced liver injury by inhibiting c-Jun N-terminal kinase activation. Gastroenterology. 2008; 135:1311–1321. [PubMed: 18700144]

Ni HM, Bockus A, Boggess N, Jaeschke H, Ding WX. Activation of autophagy protects against acetaminophen-induced hepatotoxicity. Hepatology. 2012; 55:222–232. [PubMed: 21932416]

Polson J, Lee WM. American Association for the Study of Liver Disease. AASLD position paper: the management of acute liver failure. Hepatology. 2005; 41:1179–1197. [PubMed: 15841455]

Prescott LF, Park J, Ballantyne A, Adriaenssens P, Proudfoot AT. Treatment of paracetamol (acetaminophen) poisoning with N-acetylcysteine. Lancet. 1977; 2:432–434. [PubMed: 70646]

Ramachandran A, McGill MR, Xie YC, Ni HM, Ding WX, Jaeschke H. Receptor interacting protein kinase 3 is a critical early mediator of acetaminophen-induced hepatocyte necrosis in mice. Hepatology. 2013; 58:2099–2108. [PubMed: 23744808]

Saberi B, Ybanez MD, Johnson HS, Gaarde WA, Han D, Kaplowitz N. Protein kinase C (PKC) participates in acetaminophen hepatotoxicity through c-jun-N-terminal kinase (JNK)-dependent and -independent signaling pathways. Hepatology. 2014; 59:1543–1554. [PubMed: 23873604]

Saito C, Lemasters JJ, Jaeschke H. c-Jun N-terminal kinase modulates oxidant stress and peroxynitrite formation independent of inducible nitric oxide synthase in acetaminophen hepatotoxicity. Toxicol Appl Pharmacol. 2010a; 246:8–17. [PubMed: 20423716]

Saito C, Zwingmann C, Jaeschke H. Novel mechanisms of protection against acetaminophen hepatotoxicity in mice by glutathione and N-acetylcysteine. Hepatology. 2010b; 51:246–254. [PubMed: 19821517]

Sharma M, Gadang V, Jaeschke A. Critical role for mixed-lineage kinase 3 in acetaminophen-induced hepatotoxicity. Mol Pharmacol. 2012; 82:1001–1007. [PubMed: 22918968]

Shinohara M, Ybanez MD, Win S, Than TA, Jain S, Gaarde WA, Han D, Kaplowitz N. Silencing glycogen synthase kinase-3 beta inhibits acetaminophen hepatotoxicity and attenuates JNK activation and loss of glutamate cysteine ligase and myeloid cell leukemia sequence 1. J Biol Chem. 2010; 285:8244–8255. [PubMed: 20061376]

Smilkstein MJ, Knapp GL, Kulig KW, Rumack BH. Efficacy of oral N-acetylcysteine in the treatment of acetaminophen overdose. Analysis of the national multicenter study (1976 to 1985). N Engl J Med. 1988; 319:1557–1562. [PubMed: 3059186]

Starkey Lewis PJ, Dear J, Platt V, Simpson KJ, Craig DG, Antoine DJ, French NS, Dhaun N, Webb DJ, Costello EM, Neoptolemos JP, Moggs J, Goldring CE, Park BK. Circulating microRNAs as potential markers of human drug-induced liver injury. Hepatology. 2011; 54:1767–1776. [PubMed: 22045675]

Xie YC, Williams CD, McGill MR, Lebofsky M, Ramachandran A, Jaeschke H. Purinergic receptor antagonist A438079 protects against acetaminophen-induced liver injury by inhibiting P450 isoenzymes, not by inflammasome activation. Toxicol Sci. 2013; 131:325–335. [PubMed: 22986947]

Zhang YF, He W, Zhang C, Liu XJ, Lu Y, Wang H, Zhang ZH, Chen X, Xu DX. Role of receptor interacting protein (RIP)1 on apoptosis-inducing factor-mediated necroptosis during acetaminophen-evoked acute liver failure in mice. Toxicol Lett. 2014; 225:445–453. [PubMed: 24440347]

Highlights

- APAP reproducibly causes cell death in freshly isolated primary human hepatocytes.
- APAP induces adduct formation, JNK activation and mitochondrial dysfunction in PHH
- Mitochondrial adducts and JNK translocation are delayed in PHH compared to mice
- JNK inhibitor SP600125 partially protects against APAP-induced cell death in PHH
- N-acetylcysteine provides significant protection even if administered 6h after APAP

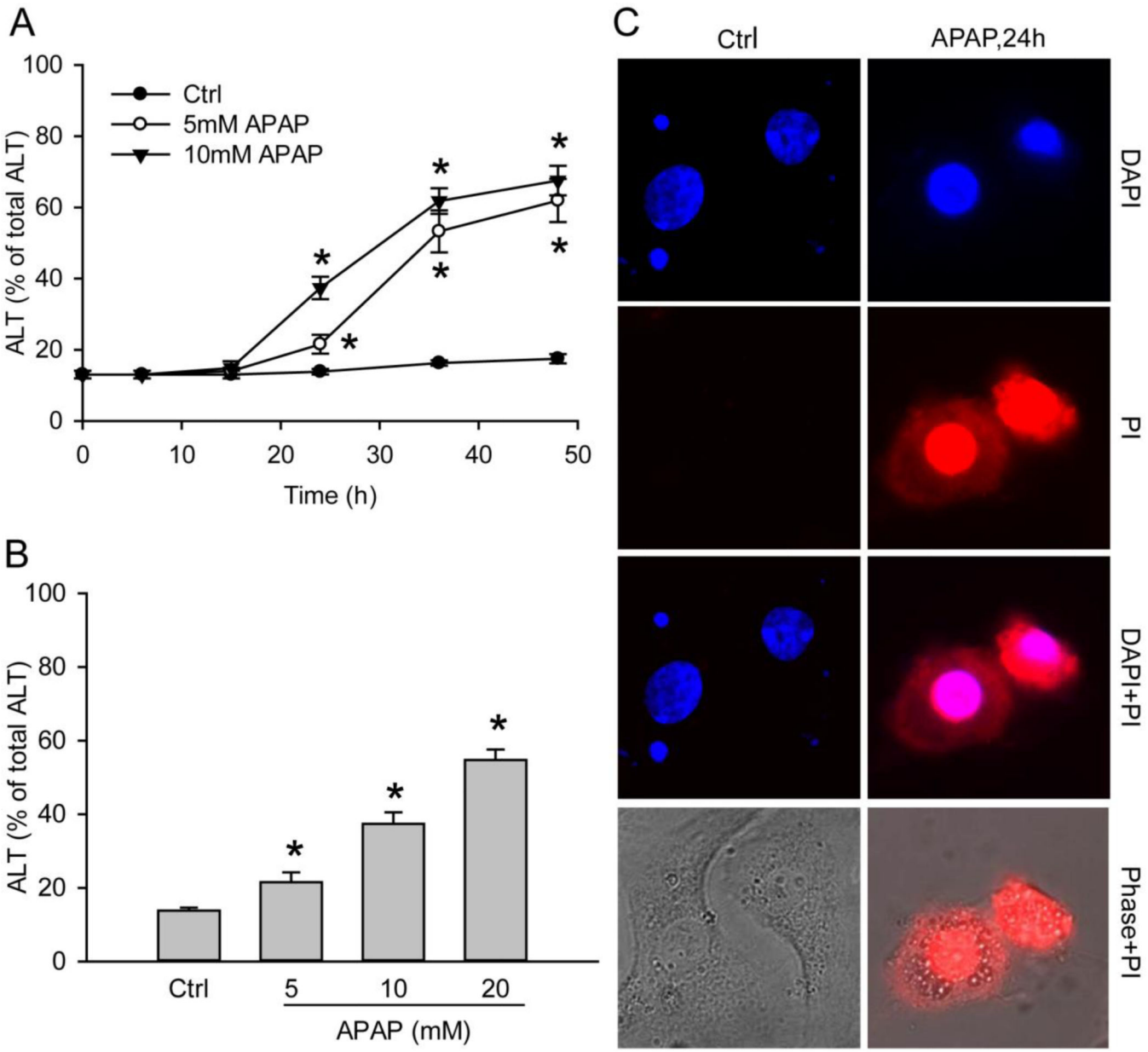

Figure 1. APAP induces cell death in primary human hepatocytes (PHH)

Cells were treated with 5mM or 10mM APAP over a period of 48 hours. (A) Time course of toxicity over 48 hours, as indicated by percentage of alanine aminotransferase (ALT) activity found in the culture medium, (B) Dose-response of APAP toxicity at 24 hours after treatment. (C) Necrotic cell death as indicated by nuclear PI staining after 24h after 10mM APAP exposure. The nucleus was stained with DAPI. Data in A and B represent mean ± SE of 20 independent cell isolations. *$P < 0.05$ (compared with time 0 or control).

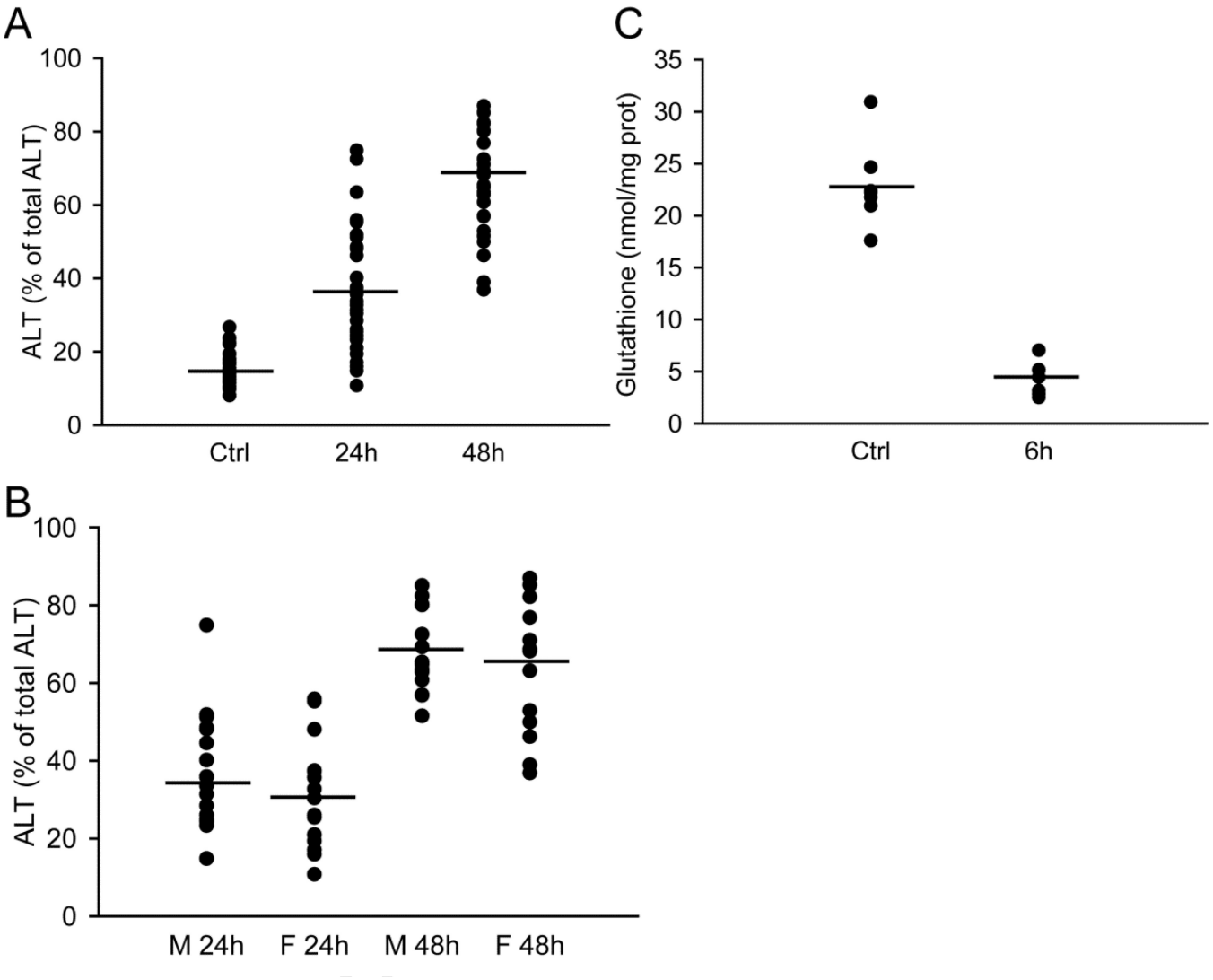

Figure 2. Inter-individual variation of ALT and GSH levels in primary human hepatocytes

(A) ALT release from hepatocytes isolated from 44 patients. Each batch of cells (individual patient) were either untreated (0), or exposed to 10mM APAP for 24 and 48 hours. (B) ALT release from hepatocytes isolated from male and female patients 24 and 48 hours after 10mM APAP. (C) GSH levels of hepatocytes from each individual (n=7) at 0 and 6 hours after 10mM APAP. Horizontal lines indicate average values.

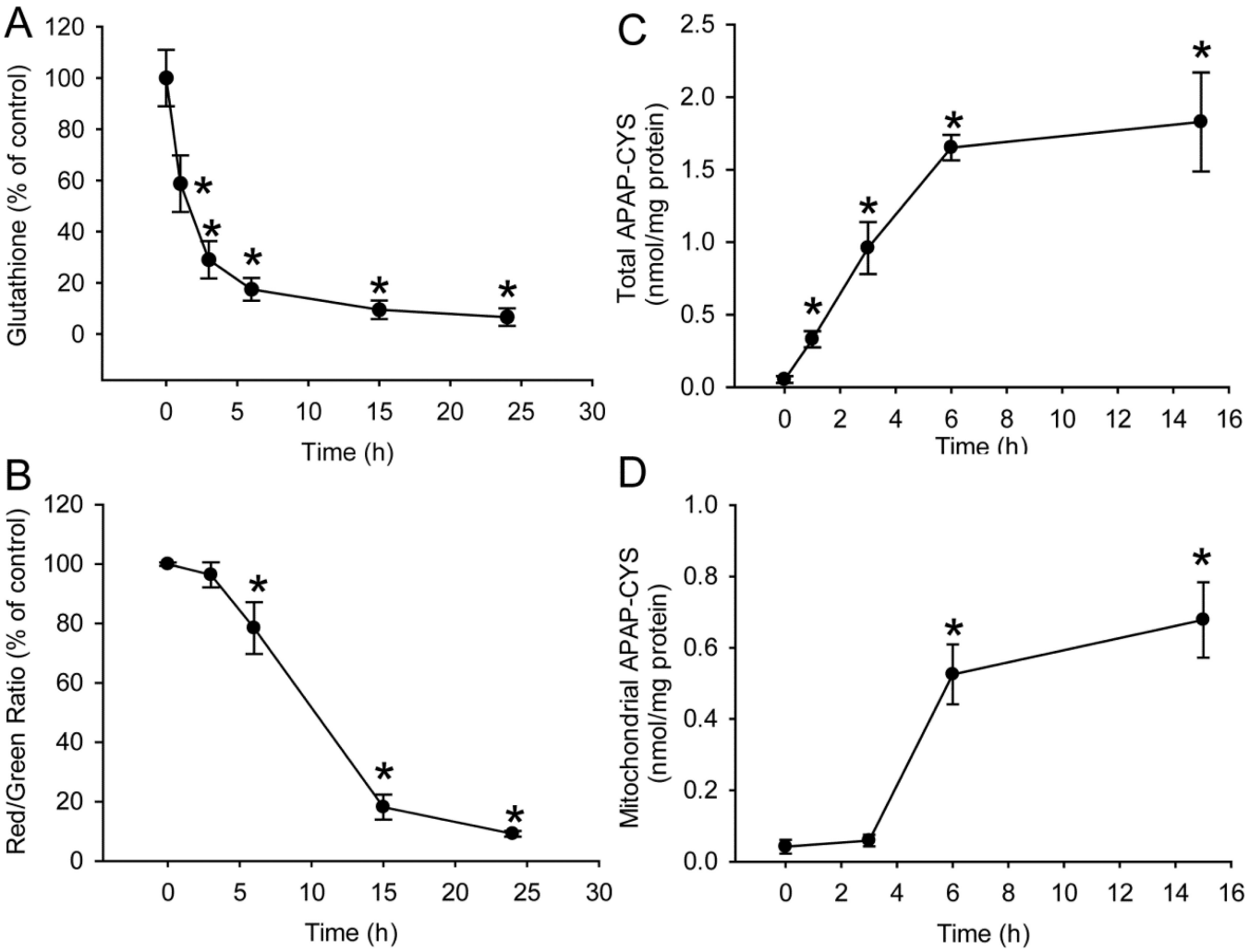

Figure 3. APAP triggers GSH depletion, mitochondria dysfunction and protein adduct formation in PHH

(A) Time course of cellular glutathione depletion after 10mM APAP. (B) Loss of mitochondria membrane potential over 24 hours after 10mM APAP, as indicated by decrease of red/green fluorescence ratio using the JC-1 assay. APAP-protein adduct formation (C) in the whole cell and (D) in the mitochondria fraction over 15 hours after 10mM APAP. Data represent mean ± SE from experiments using cells from 3–8 donors. * $P < 0.05$ (compared with time 0).

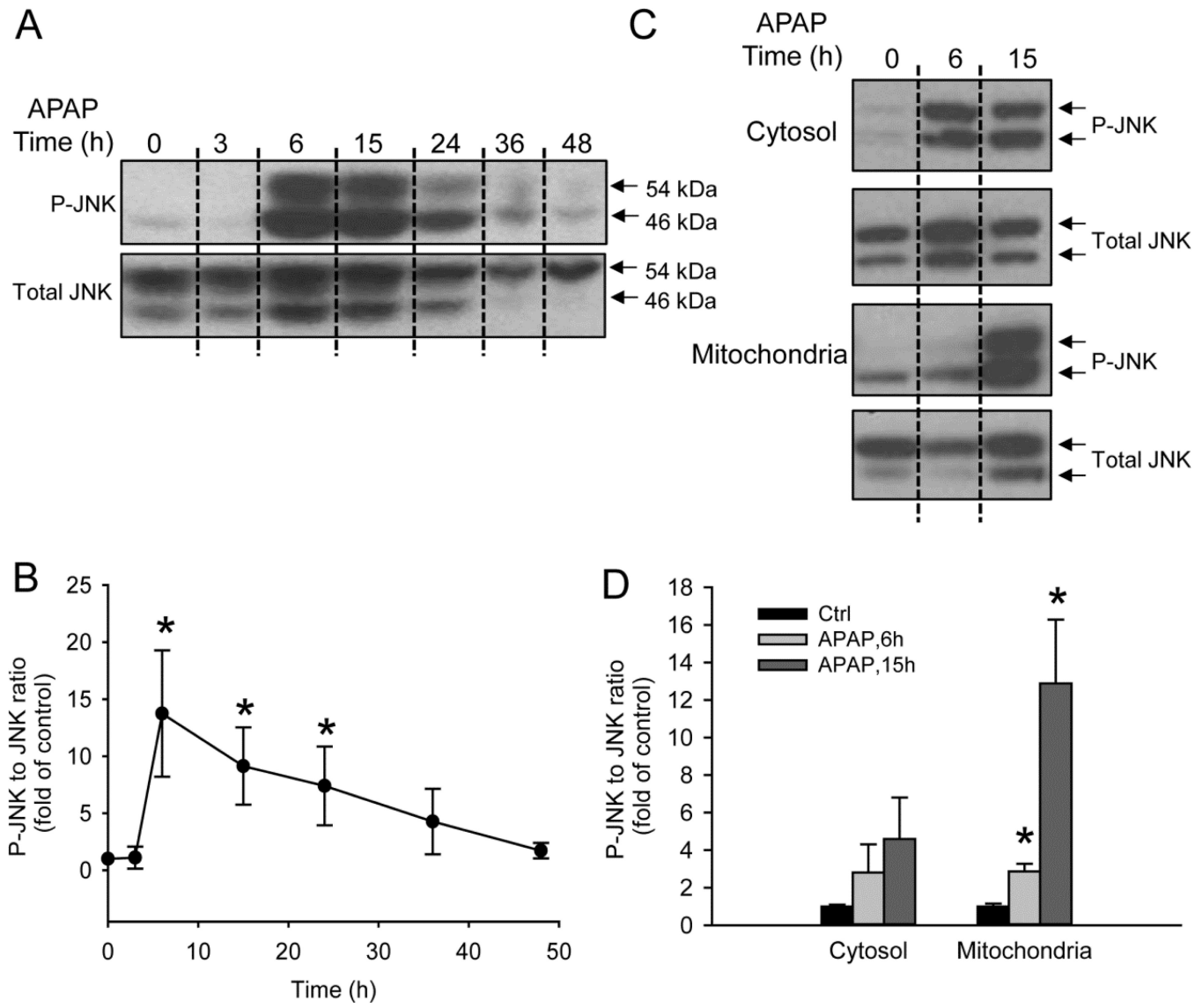

Figure 4. APAP leads to cellular JNK activation in PHH and phospho-JNK translocation to the mitochondria

(A) Time course of JNK activation in whole cell homogenate after 10 mM APAP and (B) Densitometry. (C) JNK activation in the cytosol and phospho-JNK translocation to the mitochondria and (D) Densitometry. Data represent mean ± SE of independent western blotting using PHH samples from 3–4 donors. * $P < 0.05$ (compared with controls).

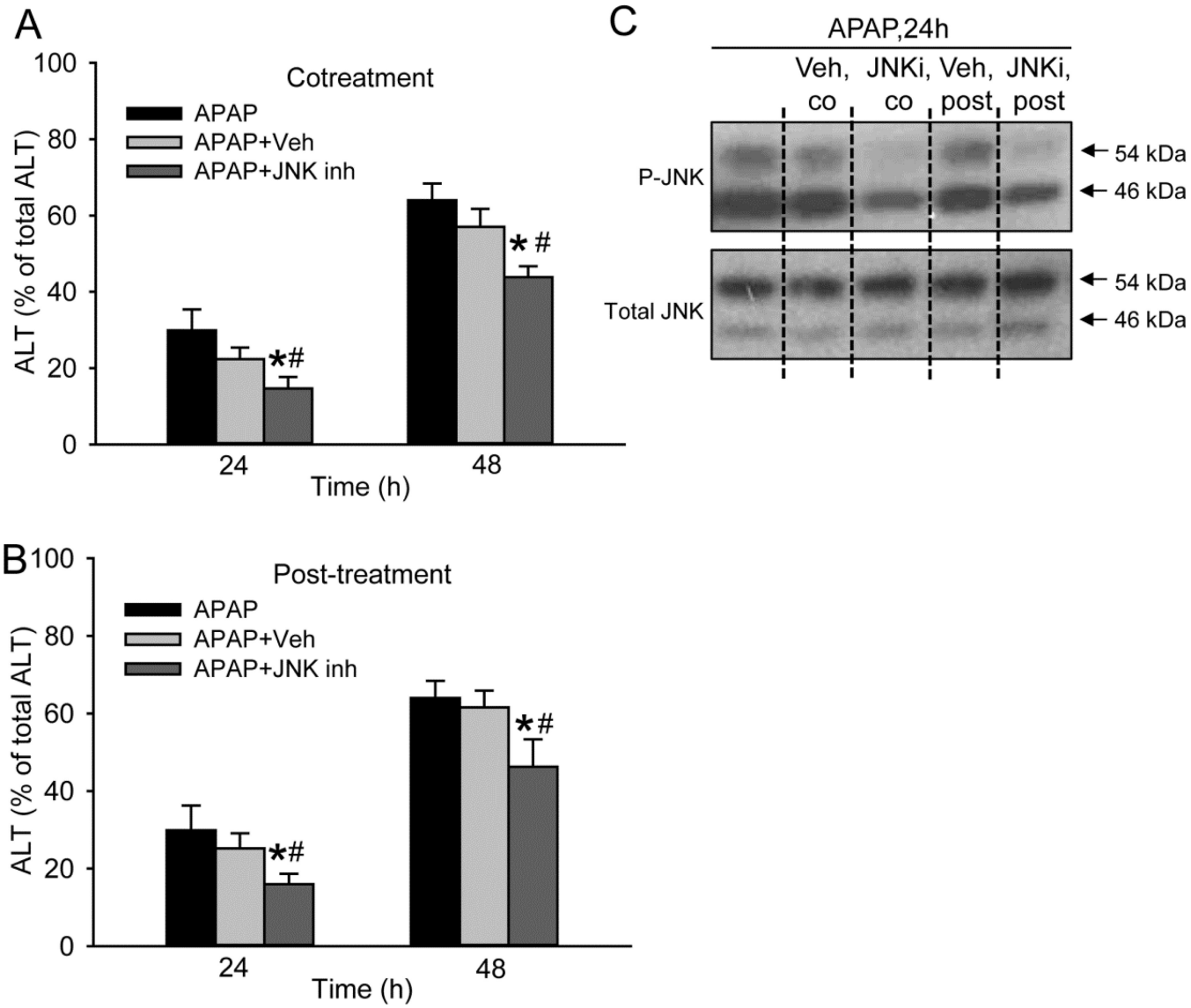

Figure 5. JNK inhibitor SP600125 partially protects against APAP-induced cell death in PHH

JNK inhibitor SP600125 using 0.2% DMSO as the vehicle was administered either as (A) a co-treatment with APAP or (B) a 3-hour post-treatment after APAP. (C) Western blotting was performed to verify the efficacy of SP600125. Data represent mean ± SE from experiments using cells from 6 donors. $^{\#}P < 0.05$ (compared with APAP+Veh group).

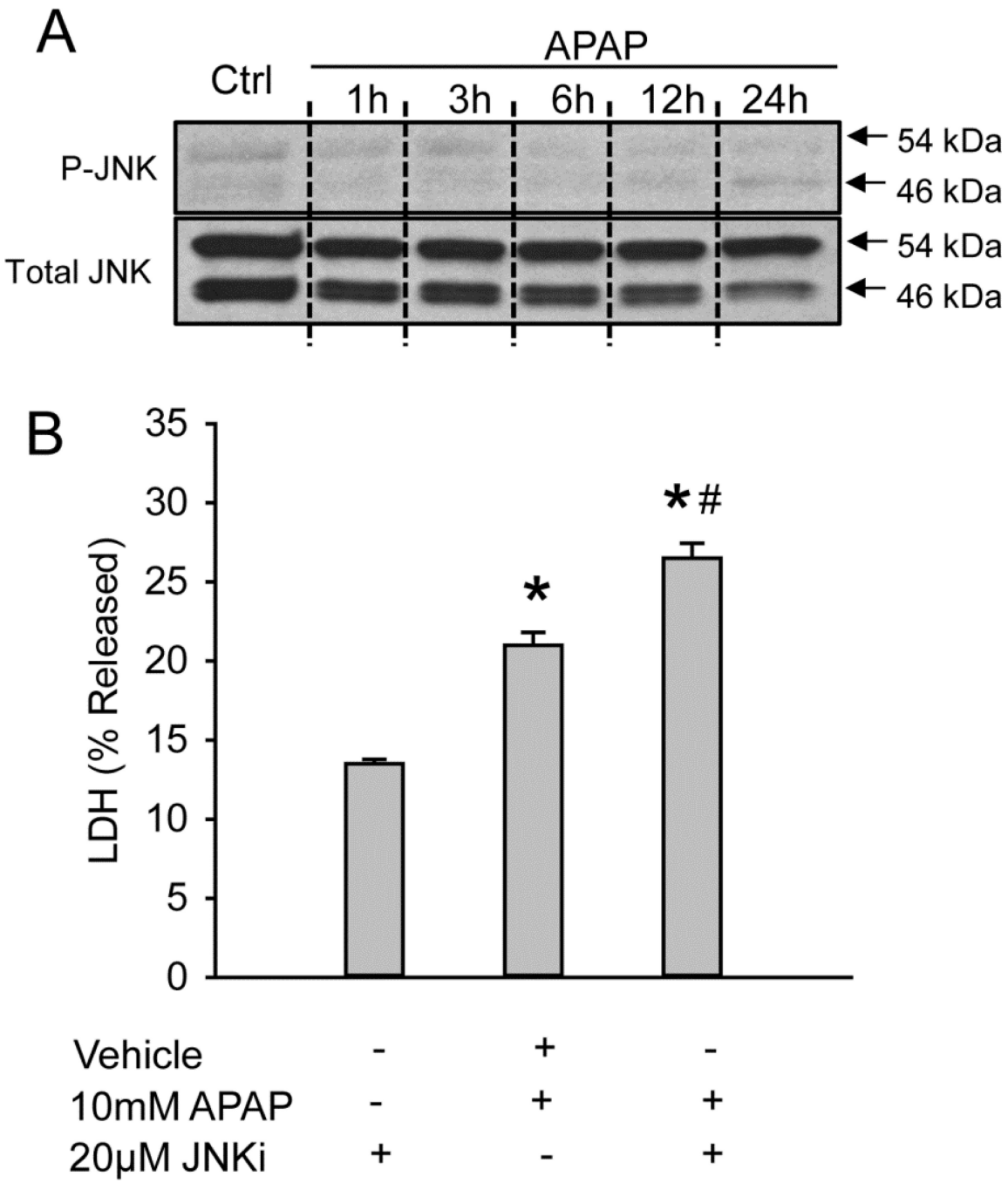

Figure 6. No JNK activation in HepaRG cells after APAP and no protection using JNK inhibitor SP600125

(A) Time course of JNK activation over 24 hours in HepaRG cells. (B) Cell death as suggested by percentage of lactate dehydrogenase (LDH) released into the culture media at 24 hours after APAP with or without JNK inhibitor SP600125 as a co-treatment. Data represent mean ± SE of n=4. * $P < 0.05$ (compared with control), $^{\#}P<0.05$ (compared with APAP group)

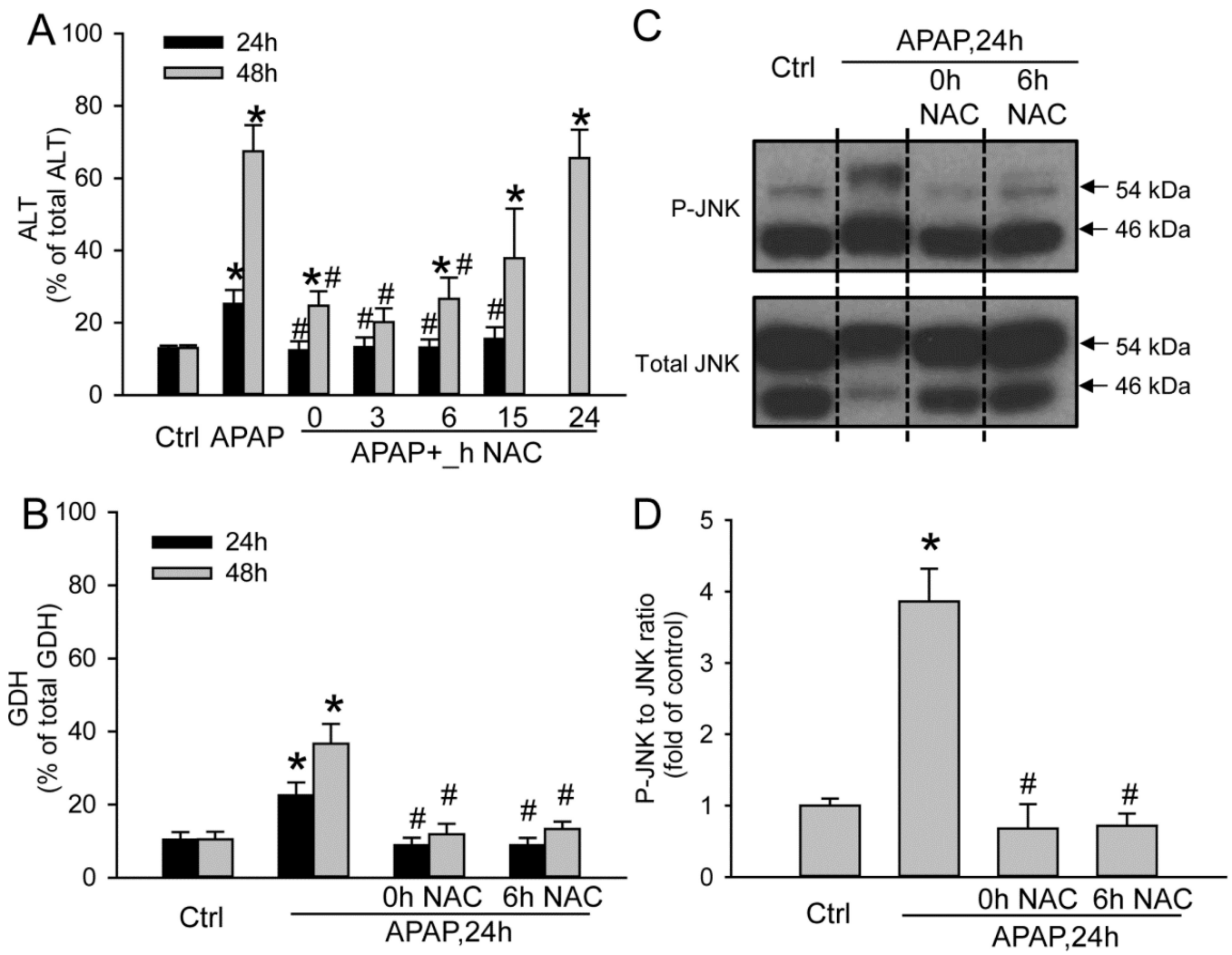

Figure 7. Protection by N-acetylcysteine (NAC) against APAP-induced hepatotoxicity in PHH

20mM NAC was applied at various time points after APAP and (A) ALT activity, (B) Glutamate dehydrogenase (GDH) activity and (C–D) JNK activation was evaluated at 24 hours or 48 hours after APAP. (D) Densitometry. Data represent mean ± SE from experiments using cells from 3–7 donors. * $P < 0.05$ (compared with control), $^{\#}P<0.05$ (compared with APAP group)

Table 1

Liver donor medical information

Criteria	Number (total=44)
Source of hepatocytes	
Resected livers	17 (39%)
Donor livers	27 (61%)
Age	
Range	23~79
Average	50.8
Gender	
Male	21 (48%)
Female	23 (52%)
Ethnicity	
Caucasian	37 (84%)
Asian	2 (5%)
Black	4 (9%)
N/A	1 (2%)
Body mass index (BMI)	
Range	21.2~49.5
Average	29.6
Smoke/Alcohol use	
Both	11 (25%)
Smoke only	6 (14%)
Alcohol only	1 (2%)
Neither	7 (16%)
N/A	19 (43%)
Diagnosis	
Metastatic colon cancer	16 (36%)
Head injury	7 (16%)
ICH/Stroke	5 (11%)
Drug overdose	4 (9%)
Cardiac arrest	4 (9%)
Asthma attack	2 (5%)
Asphyxiation/hanging	2 (5%)
Metastatic rectal cancer	2 (5%)
CVA/ Stroke	1 (2%)
SIGSW	1 (2%)

ICH; intracerebral hemorrhage

CVA; cerebrovascular accident

SIGSW; self-inflicted gunshot wounds

N/A; not available